RESEARCH PAPER

PCCP
www.rsc.org/pccp

An ultrafast excited state intramolecular proton transfer (ESPIT) and photochromism of salicylideneaniline (SA) and its "double" analogue salicylaldehyde azine (SAA). A controversial case

Marcin Ziółek,*[a] Jacek Kubicki,[b] Andrzej Maciejewski,[ac] Ryszard Naskręcki[b] and Anna Grabowska[d]

[a] *Center for Ultrafast Laser Spectroscopy, Adam Mickiewicz University, Umultowska 85 61-614 Poznan, Poland. E-mail: marziol@amu.edu.pl; Tel: +48 61 829 5011*
[b] *Quantum Electronics Laboratory, Faculty of Physics, Adam Mickiewicz University, Umultowska 85 61-614 Poznan, Poland*
[c] *Photochemistry Laboratory, Faculty of Chemistry, Adam Mickiewicz University, Grunwaldzka 6 60-780 Poznan, Poland*
[d] *Institute of Physical Chemistry, Polish Academy of Sciences, Kasprzaka 44 01-224 Warsaw, Poland*

Received 10th May 2004, Accepted 26th July 2004
First published as an Advance Article on the web 16th August 2004

Two simple, structurally related photochromic Schiff bases, salicylideneaniline (SA) and salicylaldehyde azine (SAA) were studied in femto– and picosecond time domains. In both systems an ultrafast excited state intramolecular proton transfer (ESIPT) reaction was stated with the characteristic time below 50 fs. For SA this result is in contrast to the recent data published by Mitra and Tamai (S. Mitra and N. Tamai, *Chem. Phys. Lett*., 1998, **282**, 391; S. Mitra and N. Tamai, *Chem. Phys*., 1999, **246**, 463; S. Mitra and N. Tamai, *Phys. Chem. Chem. Phys*., 2003, **5**, 4647), reporting on the corresponding time as long as 200–300 fs. The kinetics of decay of keto-tautomers in S_1 states was followed by the transient absorption (410 nm and 470 nm for SA and SAA, respectively) and stimulated emission bands. About 10–30% of excited molecules give birth to the long-lived ground states of photochromic forms.

Introduction

The excited state intramolecular proton transfer (ESIPT) processes belong to the fastest chemical reactions occurring in nature and are of great interest from both the basic and applied points of view.[1] In most cases, such a reaction follows the cycle: absorption–proton transfer–emission–back proton transfer. The last step closes the cycle, restoring the initial species, stable in the ground state. Modern ultrafast techniques, like the time-resolved laser spectroscopy, are excellent tools for the study of such processes. The phenomena of photochromism for many decades attracted much interest[2] and nowadays are also widely studied because of possible applications, *e.g*. molecular memories and switches.[3] The aromatic Schiff bases represent special group of molecular systems in which both these interesting phenomena occur. Besides the ESIPT reaction cycle, a large portion of molecules is "trapped" in the ground state as the metastable photochromic modification of the initial structure. The best known photochromic Schiff base is salicylideneaniline (SA),[4–22] shown in the Scheme 1. In the crystal state the thermochromic properties of SA were reported.[4,5] On the other hand in solution or in the isolated system its photochromism was widely studied, both experimentally[6–21] and theoretically.[6,10,14,18,19,21,22] The studies concern the mechanism and dynamics of proton transfer reaction (from the primary excited enol form to the keto tautomer) and the creation of photochromic tautomer. In spite of great efforts devoted to understanding of these mechanisms, the results are not fully consistent and much controversy is still present. One of the reasons for the complex behaviour of aromatic Schiff bases is the possible existence of many structural forms of enol, ketone and photochrome.[9,12,14,18,19,22] In recent papers[13–15] Mitra and Tamai reported the characteristic time of proton transfer process for SA in the range of 200–300 fs in different solvents. However, in our previous paper[23] we reported on much faster proton transfer rate (<50 fs) in *N*,*N*′-bis(salicylidene)-*p*-phenylenediamine (BSP), a symmetric molecule belonging to the same family as SA (see Scheme 1).

Thus, we decided to undertake the studies of SA in complementary, time-resolved (on femto- and picosecond time scale) and stationary measurements, with the same experimental setup as used earlier.[23] We chose acetonitrile (ACN) as a solvent with very low viscosity and fast solvation dynamics, which does not form hydrogen bonds (or much weaker ones than the intramolecular H-bonds in Schiff bases). The excitation wavelength was taken at the longest possible wavelength (390 nm) to deliver minimum vibrational energy excess and

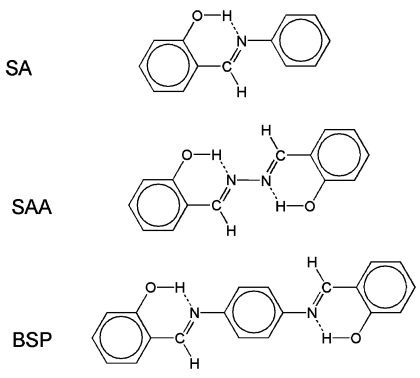

Scheme 1 Formulae of SA, SAA and BSP.

DOI: 10.1039/b406898j

make the interpretation easier. We also chose another Schiff base for comparison: the salicylaldehyde azine (SAA) (Scheme 1). This is the smallest possible aromatic Schiff base with two hydrogen bonding centers. Very little is known about SAA. In crystal state at room temperature it exists as the planar enol form,[24,25] similarly to SA. In solution, interestingly, the lifetime of the ground state of the photochromic transient was found to be nearly two orders of magnitude shorter than that for other aromatic Schiff bases[9] belonging to the same family.

Experimental

Commercially available SA (Acros) was recrystallized from pentane–ether mixture. SAA was synthesized using the standard technique, by condensation of hydrazine with salicylaldehyde, and was recrystallized from ACN. All measurements were performed at the room temperature in the dried ACN (for fluorescence, Merck, or anhydrous, Aldrich). The stationary absorption spectra were taken with UV-VIS-550 (Jasco) spectrophotometer. The steady-state fluorescence emission spectra were recorded with the spectrofluorimeter with a laser as the excitation source, which ensured high intensity and sufficient monochromaticity of the excitation beam and low level of scattered light. The fluorescence excitation spectra were recorded with a modified MPF-3 (Perkin-Elmer) spectrofluorimeter. The introduced modifications enabled the single-photon counting detection and data processing using a dual-photon counting set (Light-Scan). The spectrofluorimeter was equipped with a reference quantum counter. The MPF-3 spectrofluorimeter was also used to measure the fluorescence quantum yields.

The apparatus (actually almost the same as in the steady state emission measurement) used for time-resolved emission measurements (time correlated single photon counting-TCSPC) has been already described.[26,27] The set-up used for the transient absorption has been also described in detail earlier.[28] The output of the laser system (femtosecond titanium-sapphire) was set at 1 kHz repetition rate providing pulses between 80 and 120 fs duration, with the energy up to 1 mJ. The probe beam passed through an optical delay line consisting of a retroreflector mounted on a computer-controlled motorised translation stage and then converted to white light continuum (in a 2 mm rotating calcium fluoride plate), whose diameter was 2–5 times smaller than that of the pumping beam. A grating polychromator was used in conjunction with thermoelectrically cooled CCD camera to record the spectra.

In order to improve the signal-to-noise ratio, the transient absorption measurements were performed in two-beam geometry (probe and reference) with two synchronized choppers in the pump and probe paths, respectively. This allowed substantial elimination of the influence of the laser beam fluctuations and, consequently, measurements of much lower values of the optical density changes. With this experimental set-up, the absorbance changes (ΔA) can be measured with an accuracy of ± 0.0005 in the 300 nm to 700 nm spectral range.

The thickness of the flowing sample was 2 mm and the wavelength of the pump beam was 390 nm, with the pulse energy of 30 μJ. The measurements were performed at the magic angle of 54.7° between the polarization directions of the pump and probe beams. All the spectra analyzed were corrected for group velocity dispersion effect (GVD), according to the standard numerical scheme.[29] The chirp of white light continuum was obtained by measuring two-photon absorption (TPA) in a very thin (150 μm) BK7 glass plate. An additional contribution of dispersion (due to the front window of the sample cell) was calculated from the Sellmeier equation. The real instrumental function used for the convolution with the kinetic exponential functions was determined separately for each wavelength, taking into account the cell thickness.[30] The transient absorption signals originating from the pure solvent were subtracted from the data collected.[31] A more detailed analysis of the transient absorption data correction will be presented below.

Both transient absorption spectra and time-resolved emission were measured at concentrations 5.0×10^{-3} M for SA and 4.5×10^{-4} M for SAA to obtain the absorbance (A) of 0.3 at pump wavelength. The influence of the concentration was checked in the 3.0×10^{-4}–5.0×10^{-3} M range for SA and no changes in the shape of the stationary absorption spectra were observed.

Results

Stationary absorption and fluorescence

The stationary absorption spectra of SA and SAA in ACN are shown in Fig. 1. Similarly to the previously reported studies of *N*,*N*′-bis(salicylidene)-*p*-phenylenediamine (BSP) in ACN,[23] we observed a weak long-wavelength absorption tail (not shown) for both SA and SAA. In principle, this absorption could originate from the ground state of the keto tautomer, which was observed for SA in alcohols at room temperature [6,17] and in hydrocarbons at low temperatures.[16] However, in experimental conditions of our measurements, it is very unlikely. Thus, this weak long-wavelength absorption band could be assigned to the $S_1 \leftarrow S_0$ (n,π*) absorption of the enol tautomer. The absorption bands with maxima at 29,700 cm^{-1} (ε_{max} = 10,000 M^{-1} cm^{-1}) for SA and 28,200 cm^{-1} (ε_{max} = 23,000 M^{-1} cm^{-1}) for SAA we assigned as the transitions $S_2 \leftarrow S_0$ (π,π*). In our experiments the molecules under study were excited with $\lambda_{exc} = 390$ nm. The absorptivity coefficients at this wavelength are about 400 and 3400 M^{-1} cm^{-1} for SA and SAA, respectively.

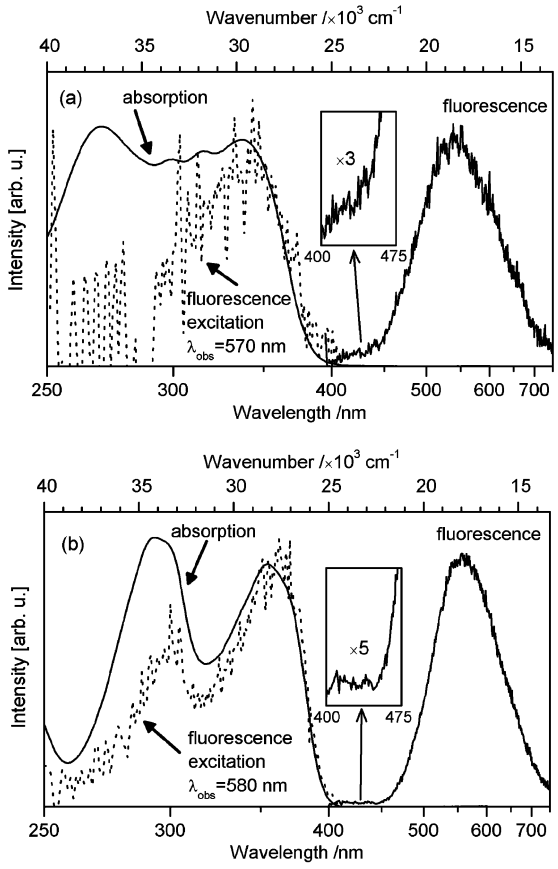

Fig. 1 The absorption, fluorescence ($\lambda_{exc} = 390$ nm) and its excitation spectra for (a) SA ($c = 5 \times 10^{-3}$ M) and (b) SAA ($c = 4.5 \times 10^{-4}$ M) in ACN. Insets: the short-wavelength emission from the enol tautomer.

Fig. 1 presents the emission spectra corrected for the sensitivity of the detection system. The dominant signal is the emission from the keto tautomer with a characteristic large Stokes shift, but the short-wavelength emission is also distinctly seen in the range of 22 000–25 000 cm^{-1}. The possibility that the short-wavelength emission might originate from the solvent impurities has been excluded. As stated previously for BSP,[23] it is highly probable that the short-wavelength emission comes from the excited enol species.

In ref. 14 the observation of fluorescence with a peak at 325 nm for excitation wavelength 280 nm was reported for SA in solution, which was ascribed to the $S_2 \rightarrow S_0$ transition. We performed the stationary measurements for excitation wavelength 270 nm, but no fluorescence was observed at $\lambda <$ 400 nm, similarly to the results in the isolated state (supersonic jet).[19]

Fig. 1 also presents the fluorescence excitation spectra. They are in good agreement with the long wavelength part of the absorption spectrum (the transition $S_2 \leftarrow S_0$ (π,π^*)) and the relative intensity is significantly lower for the transitions to higher electronic states. The fluorescence excitation spectra of SA were independent of the observation within 530–620 nm. The quantum yields of fluorescence were equal $(1.2 \pm 0.2) \times 10^{-4}$ for SA at the excitation 340–360 nm and $(0.6 \pm 0.1) \times 10^{-3}$ for SAA at the excitation 350–390 nm, using quinine sulfate in sulfuric acid[32] as the standard (see Table 1).

Time-resolved fluorescence

Dynamic measurements ($\lambda_{exc} = 390$ nm) were performed at $\lambda_{em} = 420$ nm and $\lambda_{em} = 535$ nm for SA and for $\lambda_{em} = 420$ nm and $\lambda_{em} = 550$ nm for SAA, using the TCSPC method. In the short-wavelength range of emission, the fluorescence decay time was much shorter than that in the long-wavelength range. The kinetics of the decay at $\lambda_{em} = 420$ nm for SA and SAA was identical to that of the instrument response function, hence the time of this decay was beyond the temporal resolution of the spectrofluorimeter used (<1 ps). These observations confirm that the short-wavelength emission can be accounted for by the excited state of the enol species S_2 (π,π^*), whose lifetime is shorter than 50 fs (see below). Very short fluorescence decay (~100 fs) of the enol species was also observed at short wavelength part of emission spectrum for 2-(2′-hydroxyphenyl)-4-methyloxazole in p-dioxane using the femtosecond fluorescence up-conversion method.[33] The fluorescence decay at $\lambda_{em} = 535$ nm for SA was best fitted with the bi-exponential decay model: the decay time of one component was equal to 6.7 ± 1.5 ps, and the other was of the order of several hundreds picoseconds. The fluorescence decay at $\lambda_{em} = 550$ nm for SAA was also best fitted with the bi-exponential decay with two components: the decay time of one component was equal to 19 ± 2 ps and the other was in the range of several hundreds picoseconds. The picosecond lifetime is associated with the S_1 keto state. The appearance of the small contribution of the long living component might arise from the non zero stationary concentration of the ground state of photochrome tautomer (lifetimes of the ground state of photochrome tautomer:[9] 3.5 ms for SA and 0.08 ms for SAA in ACN), generated and accumulated due to the high repetition rate (4 MHz) of the excitation pulses in our TCSPC measurements. Bi-exponential kinetics of the fluorescence decay (measured using TCSPC method) for SA in acetonitrile (7 ps and 380 ± 80 ps) was also observed by Mitra and Tamai.[14]

Transient absorption

Fig. 2 presents the time resolved absorption spectra, while Fig. 3 and Fig. 4: the kinetic curves for selected probe wavelengths for SA and SAA. The experimental kinetic curves were fitted with convolutions of mono- or bi-exponential decay with the instrumental function. The rise time of signal for all wavelengths observed is instantaneous (<50 fs, see below). The fit was performed every 5 nm in the spectral range 330–700 nm (except for the range 385–405 nm, disturbed by the pumping beam of 390 nm scattered in the direction of detection). In order to excite the primary enol form with minimum vibrational energy excess we used the 390 nm pump pulse. However, because of that we were unable to say much about the ground state depopulation dynamics, since there was almost no probing light in the spectral range below pump wavelength (because of large absorbance for $\lambda <$ 390 nm).

Within the time range of the instrumental function the amplitudes of two main bands increase: a transient absorption in the spectral range below 530 nm and a stimulated emission in the spectral range above 530 nm for both SA and SAA (Fig. 2). Below 390 nm we observed a very noisy negative signal due to the ground state depopulation for SAA. The stimulated emission bands decay monoexponentially with the characteristic times 6.8 ± 1.1 ps for SA and 20 ± 2 ps for SAA. The assignment of this decay to the S_1 state of the keto form is based on the value of the lifetime (consistent with our TCSPC measurements and earlier reports for SA)[14,15] and on the

Table 1 Photophysical parameters of SA, SAA and BSP in ACN

	SA	SAA	BSP[a]
Enol tautomer:			
$\tilde{\nu}^{abs}_{max}/cm^{-1}$	29,700	28,200	27,000
$\Delta\tilde{\nu}_{1/2}/cm^{-1}$[b]	4000	4000	4100
$\varepsilon_{max}/M^{-1}\ cm^{-1}$	10,000	23,000	35,000
$k_F/10^7\ s^{-1}$[c]	10	21	28
Lifetime/fs	<50	<50	<50
Keto tautomer:			
$\tilde{\nu}^{em}_{max}/cm^{-1}$	18,500	17,900	17,700
Lifetime/ps	7	19	10.5
ϕ_F[d]	$1.2 \pm 0.2 \times 10^{-4}$	$0.6 \pm 0.1 \times 10^{-3}$	1.0×10^{-3}
$k_F = \phi_F\ \tau^{-1}/10^7\ s^{-1}$	1.7	3.2	9.5
Photochromic form: (ground state)			
$\tilde{\nu}^{abs}_{max}/cm^{-1}$	21,100	20,500	20,200
Lifetime/ms[e]	3.5	0.08	31.

$\tilde{\nu}^{x}_{max}$: wavenumber of the maximum of absorption (x ≡ abs)/emission (x ≡ em) band, $\Delta\tilde{\nu}_{1/2}$-FWHM of the absorption band, ε_{max}-absorptivity coefficient at maximum of the first (π,π^*) absorption band, k_F-radiative rate constant, ϕ_F-fluorescence quantum yield.

[a] From ref. 23. [b] Estimated from the long-wavelength part of the (π,π^*) absorption band. [c] Calculated from the simplified Strickler–Berg relation: $k_F = \varepsilon_{max}(\tilde{\nu}^{abs}_{max})^2\Delta\tilde{\nu}_{1/2}(3.5 \times 10^8)^{-1}$. [d] Using quinine sulfate in sulfuric acid 0.2 M, $\phi_F = 0.53$ as a standard.[32] [e] From ref. 9.

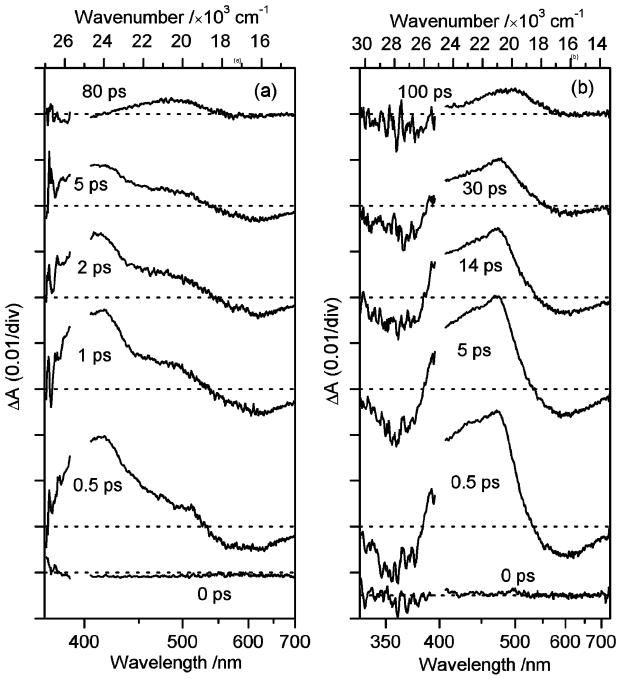

Fig. 2 Transient absorption spectra: (a) SA in ACN, $c = 5 \times 10^{-3}$ M, (b) SAA in ACN, $c = 4.5 \times 10^{-4}$ M.

occurrence of a relatively strong emission signal known to originate in the stationary measurements almost exclusively from the keto form. The position of the stationary emission band corresponds to that of the stimulated emission, taking into account that the latter is disturbed by the neighboring transient absorption band.

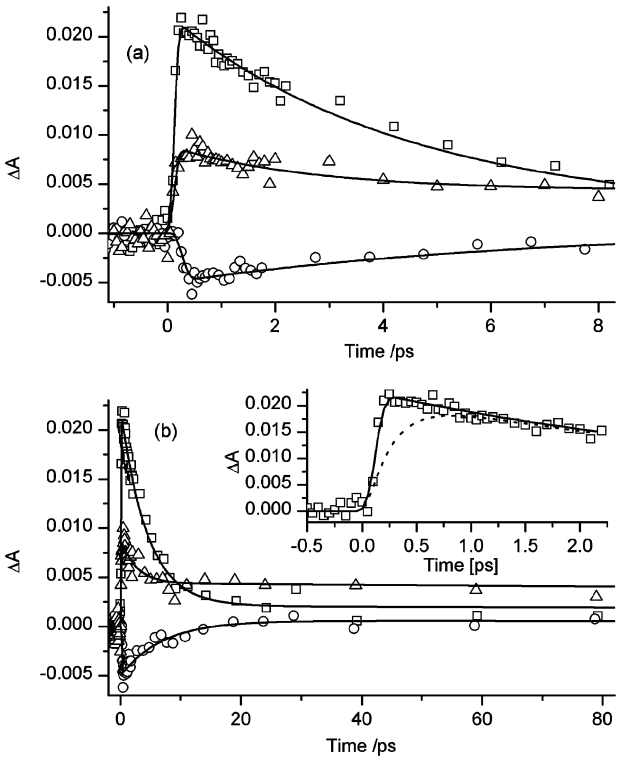

Fig. 3 Examples of the kinetic curves of the transient absorption signals for SA in ACN, and the fits in the short (a) and long (b) time scale for: 420 nm (squares), 470 nm (triangles) and 620 nm (circles) convoluted with the instrumental function. Inset: The rise of the transient absorption signal at 420 nm (squares) and fit of instantaneous rise time (solid line) and 240 fs rise time (dotted line) convoluted with the instrumental function.

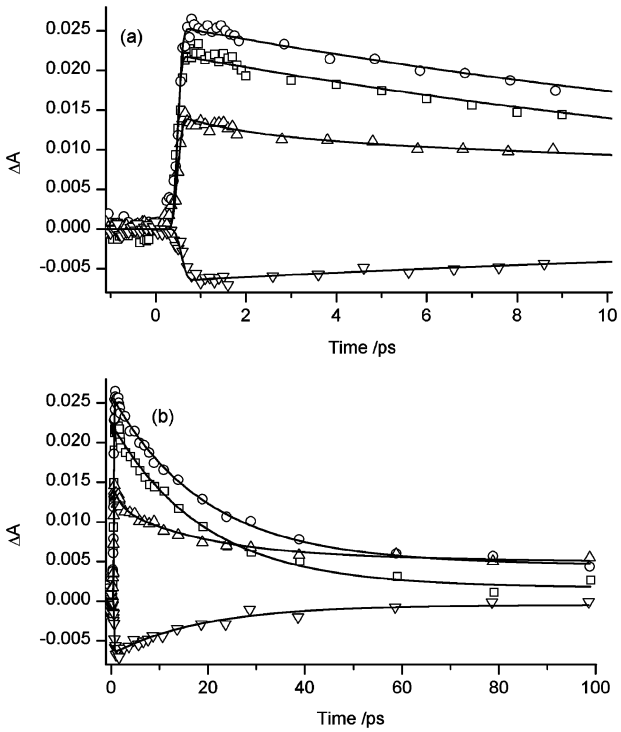

Fig. 4 Examples of the kinetic curves of the transient absorption signals for SAA in ACN, and the fits in the short (a) and long (b) time scale for: 430 (squares), 475 nm (circles), 500 nm (triangles), and 600 nm (reversed triangles) convoluted with the instrumental function.

Unlike the previously studied BSP molecule,[23] we did not observe any ultrafast decaying signal of the originally excited state in enol form. The stimulated emission and absorption bands of the S_1 keto state rise within the temporal duration of the instrumental function. Therefore, it is reasonable to estimate the proton transfer characteristic time below 50 fs. The proton transfer may be even faster than in BSP, having in mind that the signal of duration much shorter than the duration of the instrumental function has smaller experimentally observed amplitude than the real amplitude. Thus, if the signal duration is short enough, it may not be detectable although its real amplitude is comparable to other measured signals.

In contrast to stimulated emission the decay of transient absorption for SAA is clearly bi-exponential with a faster component between 1 to 3 ps and a slower component close to the lifetimes obtained by TCSPC measurements. When we fixed the decay time of the longer component at the value 19 ps, we obtained in the fitting procedure the more precise estimate of the faster component, 1.6 ± 0.2 ps. Thus, the main contribution (80–90%) comes from the 19 ps decay, and we assigned this transient absorption to the same species as that responsible for stimulated emission bands: the S_1 state of the keto form. The origin of the faster component is not yet clear for us and will be discussed below. In the case of SA it is impossible to unambiguously conclude, whether the transient absorption band decays mono- or bi-exponentially. The mono-exponential fit gives the decay time faster by about 2 ps than the decay time of the stimulated emission band. However, when we perform the bi-exponential fit for transient absorption band with two fixed parameters: longer decay component of 7 ps (decay of the S_1 state of the keto form, taken from TCSPC measurements and stimulated emission) and faster decay component below 2 ps, the same fitting quality as for the mono-exponential case was obtained. Thus, it seems more probable that SA behaves similarly to SAA and the decay is bi-exponential.

The residual transient absorption bands with a maximum at 490 nm for SAA and 480 nm for SA do not change in the time

range 100 to 1000 ps, and they are assigned to the long-lived ground state of photochrome tautomer. These transient absorption spectra of the photochromic tautomer are in very good agreement with the spectra recorded 15 ns after excitation, measured earlier with a nanosecond spectrometer.[9]

As mentioned before, the ground state depopulation band (enol tautomer) of SAA is very noisy because of high value of absorbance for wavelength shorter than 390 nm (*e.g.* $A_{390nm} = 0.3$, $A_{360nm} \sim 2$) and only a qualitative result could be obtained from mono-exponential fit $A_0 + A_1\exp(-t/\tau)$ of the signal averaged in the broad range 340–370 nm (A_0 is the amplitude of the ground state depopulation band at $t \rightarrow 100$ ps while $A_1 + A_0$ is the amplitude of the ground state depopulation band at $t = 0$). The decay time value $\tau = 23 \pm 4$ ps is in agreement with the characteristic time of the S_1 keto state. Assuming the same transient absorption cross sections of S_1 keto state and photochromic form in this spectral region, we may conclude (from the ratio of amplitudes $A_0/(A_0 + A_1) = 0.2$) that about 20 ± 10% of excited SAA molecules undergo the transformation from S_1 keto-tautomer to photochromic form, while the rest returns to the initial enol form (probably *via* the vibronically excited S_0 keto state, similarly as in the case of BSP).[23]

Another confirmation of the existence of the three kinetic components comes from the global singular value decomposition (SVD) analysis. The number of singular values, which differs from the noise, is equal to the number of transient species participating in the spectral changes.[34–36] Our SVD analysis performed for SAA in the spectral range 405–700 nm and temporal range 1–100 ps, gives three singular values (1.32, 0.15 and 0.11) significantly greater than the noise of the level of 0.05. In the case of SVD analysis of SA, the third singular value is not so well separated from the noise (singular values: 0.85, 0.14, 0.06, noise level 0.04). We were not able to apply the SVD analysis for the temporal range from 0 ps (together with the rise of the signals), as proposed in ref. 36 because in the case of 2 mm sample cell the instrumental response function is significantly wavelength dependent (which will be also presented in the discussion below).

In principle, if the bands change their shape (a shift of peak position or a spectral narrowing), the SVD analysis fails, since it gives a series of many decreasing singular values. However, the simulations performed by us revealed that, in the case of our signal to noise ratio, the possible spectral changes due to vibrational relaxation would result in only one additional singular value greater than the noise. Thus, the "hot" state acts as one separate transient species, which was also assumed in the SVD analysis of the similar system (2,5-bis(2′-benzoxazolyl) hydroquinone, BBHQ, denoted sometimes as BBXHQ) in ref. 36.

Discussion

Most of our time resolved data for SA in ACN, the transient absorption spectra and fluorescence decay times, are in agreement with the results presented for the same system with similar experimental tools by Mitra and Tamai.[13–15] However, some of our observations are contrary to their results, especially the characteristic time of the excited state proton transfer, which was reported to be 240 fs for SA in ACN.[14,15] This important point needs some methodological discussion. The time of 240 fs was obtained by fitting the rise time to the kinetics measured at the most intense band of transient absorption (420 nm) of the S_1 state of the keto form. In our case the rise time was instantaneous (in the whole transient absorption and stimulated emission region–see inset in Fig. 3b). Thus, we concluded that the proton must be transferred in less than 50 fs. All our fits of the kinetic curves involved the temporal instrumental function taking into account the cell thickness and hence the dispersion of the delay between the pump and the probe (originating from different group velocities of pump and probe pulses in the sample). The pump–probe cross correlation function unaffected by dispersion was determined basing on the two-photon absorption in BK7;[30] its FWHM is 150 fs. The real instrumental function used for the convolution with the kinetic exponential functions was determined separately for each wavelength, according to the theory presented in ref. 30. Fig. 5 shows the examples (for different wavelengths) of the calculated pump–probe cross correlation function (the instrumental function) for 2 mm sample cell filled with ACN solvent. The increase of the difference between probe and pump wavelengths causes broadening of the temporal instrumental function. In the refs. 13–15 there is no information about the determination of the pump–probe cross correlation function, and we suppose that the time of their instrumental function might be underestimated. This may lead to overestimated rise time.

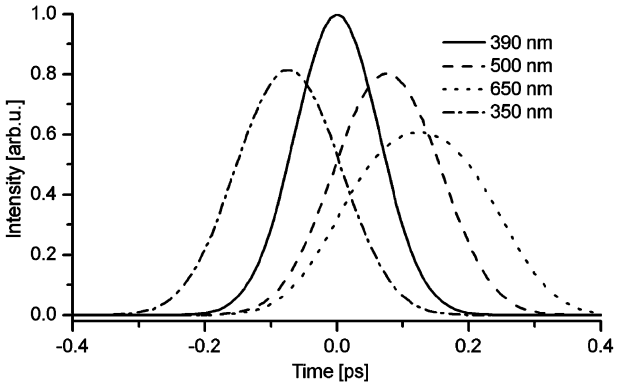

Fig. 5 The instrumental function calculated for different probe wavelengths, for pump wavelength 390 nm.

Moreover, the temporal maximum of the instrumental function changes to more positive time delays as the wavelength increases (Fig. 5), which has nothing to do with the chirp of the probe pulse (the latter causes the same effect but can be easily corrected as presented in the Experimental section). In refs. 13–15 the sample has the same thickness as ours (2 mm), but the pump wavelength is shorter (360 nm), which even increases the delay time. Thus, it is difficult to compare the transient absorption bands in the broad spectral regime during the initial growth of their amplitude, when they are convolved with the instrumental function. Particularly, the stimulated emission observed at the wavelengths >580 nm some 200–300 fs later than the transient absorption at shorter wavelength[13–15] might be explained not by the delay of the S_1 keto state emission (due to the ESIPT) but by the wavelength dependent temporal shift (and broadening) of the instrumental function. The same concerns the delayed appearance of the shoulder at around 485 nm.[13,15]

Finally, the broad spectrum in the wavelength region 400–500 nm (observed just after excitation) assigned to the primary excited enol form[13,15] is questionable for one more reason. In the time range of the pump–probe overlap, some transient absorption signals appear assigned to non-linear interaction between the pure solvent and the pump pulse.[31] For many wavelengths (especially <500 nm) these signals are comparable with the measured SA and SAA signals. In order to obtain true undisturbed response, coming only from the compounds studied, we also measured (in the same experimental conditions) the signal from the pure solvent, which was then appropriately subtracted from the data collected, as proposed in ref. 31. Since in refs. 13–15 there are no references to solvent signals or their subtraction, the initial broad spectrum can originate from the two-photon absorption or cross phase modulation in acetonitrile.

Another confirmation of the ultrashort ESIPT reaction with the characteristic time of <50 fs rather than 200–300 fs are the results of the latest measurements on the system of similar size,

which also undergoes the ESIPT reaction, namely HBT (2-(2′-hydroxyphenyl)benzothiazole). The analysis of transient absorption measured both in the visible (electronic transitions) and infrared spectral ranges (vibrational transitions) of probing wavelength indicate that the proton transfer occurs in the time range of 30–50 fs.[1,37–39] The studies of the transient absorption oscillatory features caused by the wavepacket evolution[38,39] together with detailed theoretical calculations[40] revealed that the main contribution to the proton transfer reaction mechanism comes from the low frequency skeletal vibrations of the molecule. The low frequency modes modulating the distance between the oxygen and nitrogen atoms promote the proton transfer by lowering the potential barrier for this process, and since then they determine its time scale. They also act as accepting modes of the energy excess in the keto configuration. Similar prominent role of low frequency modes was observed for other molecular systems which undergo ESIPT reaction: TIN (2-(2′-hydroxy-5′methylphenyl) benzotriazole)[41] and BBHQ.[36] In our study we were not able to resolve the oscillatory behavior of the transient absorption signal because of longer pulse duration, but we think that the proton transfer mechanism in SA and SAA molecules should be very similar to that proposed for HBT.

Moreover, in ref. 19 the laser induced fluorescence spectrum of jet-cooled SA was presented, and the 200–300 fs characteristic time of the proton transfer process was not sufficient to explain the broad feature of that spectrum. Upon assumption of the shorter (<50 fs) lifetime of the primary excited SA enol form, the homogeneous broadening of vibronic bands can be accounted for by the ESIPT reaction.

We neither observed the spectral narrowing, nor the blue shift of the transient absorption band of the proton-transferred form between 0.4 and 0.8 ps after excitation, as reported in refs. 13–15, which was interpreted as due to the intramolecular vibrational redistribution (IVR) in the hot S_1 state of the keto tautomer. This apparent contradiction may be, however, explained by the different excitation wavelength used by us (390 nm) and Mitra and Tamai (360 nm).[13–15] As a result, in our case the vibrational energy excess is much smaller and the IVR process is less pronounced. It should not be also totally excluded that the different excess of vibrational energy might cause the different characteristic time of ESIPT and this could explain the discrepancy between the results from refs. 13–15 and ours. However, in the measurements of TIN molecule[42] no influence of the excitation wavelength on the proton transfer rate constant is observed.

As mentioned in the previous section, the fast decay component (< 2 ps) in transient absorption bands of SA and SAA has not been reported in refs. 13–15 and its origin is not clear to us. The fast decay component is neither present in the evolution of stimulated emission bands nor in the time resolved fluorescence measurements. The transient species connected with this component could be populated parallel to the S_1-keto tautomer or S_1-keto could be formed from this fast decaying transient species.

One candidate for the parallel population is the (n,π*) enol state excited by the 390 nm pump pulse, from which the emission can be neglected. Usually the initial excitation of the (n,π*) state is of minor importance because of low absorptivity coefficients compared to the (π,π*) state. However, in our experiments the excitation with 390 nm corresponds to the red tail of the main (π,π*) absorption, where the absorptivity coefficient is low. From the theoretical calculation for SA[22] the (n,π*) state is located in the vicinity of the first strong (π,π*) transitions. Similar location of the (n,π*) and (π,π*) states for SAA was obtained in this work using the semiempirical calculations.[43,44] Thus, the contribution of the (n,π*) excitation may be not negligible and could explain the lack of the fast decay component for SA when the shorter excitation wavelength is used.[13–15]

Another explanation for the fast component may be the existence of two keto conformers in their S_1 state: one of them decays in the time scale of <2 ps and the second in 7 ps for SA and 19 ps for SAA. Such two keto conformers with similar energies in the excited state were theoretically predicted for SA in ref. 22 and in ref. 19: one of them is planar and the second is twisted. They could be populated parallel, and the one with shorter lifetime could have much smaller radiative rate constant and thus not be detectable in emission. These two keto conformers might also be consecutive photoproducts, according to prediction of ref. 22. Barbara *et al.*[7] observed two different components of the SA fluorescence at 4 K in various solvents and they concluded that the short living species is the precursor of the longer living one. At the room temperature in aprotic solvents they observed only one component, and they postulated that the faster component was shorter than their time resolution (5 ps). In our case, however, the lack of the faster decay component in the stimulated emission region implies that the emission cross sections ratio of shorter and longer living keto conformers should be constant in the whole 550–700 nm wavelength range, which seems rather improbable.

Finally, the explanation of the fast component of 1–2 ps duration might be solvent assisted vibrational relaxation of the hot S_1 keto state. Similar time scales of this process for analogous systems were reported in ref. 37, 45 and 46. The spectral shift of infrared peaks of the keto state of HBT molecule was assigned to IVR (several hundreds of femtoseconds) and cooling (10–20 ps),[37,45] whereas the 2.5 ps decay component of the fluorescence from 1-hydroxyanthraquinone molecule was assigned to vibrational cooling.[46]

It has been previously assumed for SA[6,7,13–15] the common precursor of the photochromic transient and the emitting keto tautomer to be the vibrationally excited "hot" keto form. We were not able to observe directly the rise of photochrome transient absorption signal because it overlaps with the transient absorption of keto tautomer in S_1 state and stimulated emission band; additionally the amplitude of two latter bands are greater than this of photochrome. However, since in the whole spectral range we observed only three kinetic processes (below 50 fs, below 2 ps and 7 ps), the creation of the photochromic transient must be hidden in one of them. The creation of photochrome in S_0 state within 50 fs is highly improbable because this process is accompanied by the significant change of the conformation of molecule.[12,22] The dynamics below 2 ps also should not be connected with the rise of photochromic band because this fast component has positive amplitudes in the whole spectral range (the decay of signals) and is absent in the evolution of the signals in the 520–560 nm range, where the photochrome transient absorption dominates. Thus, it seems most probable that the photochrome of SA (as well as SAA) is populated mostly from the relaxed S_1-keto state with the characteristic time of 7 ps for SA and 19 ps for SAA. The two-step laser induced fluorescence of SA in ACN, assigned to the emission of photochromic form,[10] was not observed in the isolated state.[19] This may even suggest that photochromic transient is not created when the vibrational relaxation to the relaxed S_1-keto state is strongly suppressed.

It should be noted that the observations of bimodal kinetics of fluorescence measurements in ref. 7 are not the direct evidence for the common precursor of the photochromic transient and the fluorescent keto tautomer since they only reveal the dynamics in the keto form. Another argument was the observation of decreasing quantum yield of keto fluorescence and simultaneous increasing the yield of creation of photochrome with decreasing excitation wavelength[6] (with respect to the 365 nm excitation). However, for wavelength used in ref. 6 (365, 334, 313, 254 nm) the excitation to the higher electronic states of the enol form should be considered and very likely the deactivation scheme is different then. Perhaps, the photochrome transient may be also populated

omitting the fluorescent (S_1) keto state. It is also consistent with significant lowering of intensity of fluorescence upon excitation to higher electronic states ($\tilde{\nu} > 30\ 000\ cm^{-1}$, Fig. 1). In ref. 47 the decrease of fluorescence intensity of methyl salicylate (the most often studied organic molecule showing ESIPT reaction) with increasing excitation energy was discussed in terms of dissociation of hydrogen bond for sufficient vibrational energy excess. In our case, such a breaking of the hydrogen bond might lead to the formation of photochromic transient in a competitive channel to that *via* the relaxed S_1 keto state.

Knyazhansky[12] has shown that in the structural modification of SA containing the "bridge" preventing the rotation of salicylidene ring the fluorescence quantum yield strongly increases, and the photochromic transient is not created. However, according to our studies (this work and ref. 23) only 10–30% of molecules are transformed to the photochromic transient. This suggests that other "twisting" changes have to be added to the scheme of nonradiative deactivation channels of S_1-keto state.

The comparison of photophysical properties of three Schiff bases which we investigated: SA, SAA (studied in this article) and BSP (studied in ref. 23) is shown in Table 1. Extending the size of the molecular π-electron system (SA → SAA → BSP) results in the red-shifting of the absorption band, increasing the absorptivity coefficient for stationary enol absorption and increasing the radiative rate constant for both enol and keto tautomers. Our value of fluorescence quantum yield for SA in ACN is in agreement with that reported in ref. 14 ($\sim 10^{-4}$) and in ref. 20: 0.7×10^{-4} in cyclohexane (CHX), 2.1×10^{-4} in ethanol (EtOH) and 2.3×10^{-4} in butanol (BuOH). The lifetimes of the S_1-keto state of SA reported for different solvents in ref. 20 are significantly longer than those measured by two independent techniques in ref. 14 (which is in agreement with our lifetime in ACN). Thus, taking the quantum yields from ref. 20 but the lifetimes from ref. 14 the radiative rate constant of keto tautomer of SA can be calculated for other solvents as follows: $1.7 \times 10^7\ s^{-1}$ for CHX, $1.9 \times 10^7\ s^{-1}$ for EtOH and $0.9 \times 10^7\ s^{-1}$ for BuOH. These values are similar to our value in ACN.

Conclusions

The following scheme of deactivation of the SA and SAA molecules in ACN was determined on the basis of the time-resolved transient absorption and emission measurements on the pico– and femtosecond time scale as well as of the stationary absorption and emission measurements in the visible and in the near UV range. The excitation to the S_2 (π,π^*) enol state is followed by a very fast (<50 fs) proton transfer. As a result, all or almost all excited molecules form the keto-tautomers in S_1 state with a lifetime of 7 ps for SA and 19 ps for SAA. No transient absorption from the primary excited enol state was observed. The keto-tautomer is characterised by the stimulated emission and by the absorption band with the maximum at 410 nm for SA and 470 nm for SAA. Additional short-living (1–2 ps) feature, although not precisely assigned, may be the indication of the existence of different conformers of the keto-tautomer. About 10–30% of the molecules undergo a transition from the relaxed S_1 state of keto-tautomer to the long-lived ground state of the photochrome (the transient absorption spectrum with the maximum at 475 nm for SA and 490 nm for SAA at t → 100 ps). The rest of the molecules deactivate to the initial enol tautomer *via* the keto tautomer (vibrationally excited) in the ground state.

Acknowledgements

This work was done under financial support of the KBN (State Committee for Scientific Research) project 2 P03B 015 24. Dynamics studies were performed at the Center for Ultrafast Laser Spectroscopy at the A. Mickiewicz University in Poznan. E. Nosenko, MPh, is kindly acknowledged for performing semiempirical calculations.

References

1 *Ultrafast Hydrogen Bonding Dynamics and Proton Transfer Processes in the Condensed Phase*, ed. T. Elsaesser and H. J. Bakker, Kluwer Academic Publishers, Dordrecht, 2002.
2 E. Hadjoudis, in *Photochromism: Molecules and Systems*, ed. H. Dürr and H. Bouas-Laurent, Elsevier, Amsterdam, 1990, p. p. 685.
3 M. Irie, *Chem. Rev.*, 2000, **100**, 1683, special issue on Photochromism: Memories and Switches.
4 M. D. Cohen, G. M. Schmidt and S. J. Flavian, *J. Chem. Soc.*, 1964, 2041.
5 T. Sekikawa, T. Kobayashi and T. Inabe, *J. Phys. Chem. A*, 1997, **101**, 644.
6 T. Rosenfeld, M. Ottolenghi and A. Y. Meyer, *Mol. Photochem.*, 1973, **5**, 39.
7 P. F. Barbara, P. M. Rentzepis and L. E. Brus, *J. Am. Chem. Soc.*, 1980, **102**, 2786.
8 K. Kownacki, Ł. Kaczmarek and A. Grabowska, *Chem. Phys. Lett.*, 1993, **210**, 373.
9 K. Kownacki, PhD Thesis (in Polish), Institute of Physical Chemistry, Polish Academy of Sciences, Warsaw, 1994.
10 K. Kownacki, A. Mordziński, R. Wilbrandt and A. Grabowska, *Chem. Phys. Lett.*, 1994, **277**, 270.
11 A. Grabowska and K. Kownacki, *Acta Phys. Pol. A*, 1995, **88**, 1081.
12 M. I. Knyazhansky, A. V. Metelitsa, A. Ya. Bushkov and S. M. Aldoshin, *J. Photochem. Photobiol. A*, 1996, **97**, 121.
13 S. Mitra and N. Tamai, *Chem. Phys. Lett.*, 1998, **282**, 391.
14 S. Mitra and N. Tamai, *Chem. Phys.*, 1999, **246**, 463.
15 S. Mitra and N. Tamai, *Phys. Chem. Chem. Phys.*, 2003, **5**, 4647.
16 K. Ogawa, J. Harada, T. Fujiwara and S. Yoshida, *J. Phys. Chem. A*, 2001, **105**, 3425.
17 V. Vargas and L. Amigo, *J. Chem. Soc. Perkin Trans. 2*, 2001, 1124.
18 M. I. Knyazhansky, A. V. Metelitsa, M. E. Kletskii, A. A. Millov and S. O. Besugliy, *J. Mol. Struct.*, 2000, **526**, 65.
19 N. Otsubo, Ch. Okabe, H. Mori, K. Sakota, K. Amimoto, T. Kawato and H. Sekiya, *J. Photochem. Photobiol. A*, 2002, **154**, 33.
20 V. Vargas, *J. Phys. Chem. A*, 2004, **108**, 281.
21 M. E. Kletskii, A. A. Millov, A. V. Metelitsa and M. Knyazhansky, *J. Photochem. Photobiol. A.*, 1997, **110**, 267.
22 M. Z. Zgierski and A. Grabowska, *J. Chem. Phys.*, 2000, **112**, 6329.
23 M. Ziółek, J. Kubicki, A. Maciejewski, R. Naskręcki and A. Grabowska, *Chem. Phys. Lett.*, 2003, **369**, 80.
24 G. Arcovito, M. Bonamico, A. Domenicano and A. Vaciago, *J. Chem. Soc. B*, 1969, 733.
25 X. Xu, X. You, Z. Sun, X. Wang and H. Liu, *Acta Crystallogr., Sect. C*, 1994, **C50**, 1169.
26 J. Karolczak, D. Komar, J. Kubicki, M. Szymanski, T. Wrozowa and A. Maciejewski, *Bull. Pol. Acad. Sci.: Chem.*, 1999, **47**, 361.
27 J. Karolczak, J. Kubicki, D. Komar, T. Wrozowa, K. Dobek, B. Ciesielska and M. Maciejewski, *Chem. Phys. Lett.*, 2001, **344**, 154.
28 A. Maciejewski, R. Naskrecki, M. Lorenc, M. Ziolek, J. Karolczak, J. Kubicki, M. Matysiak and M. Szymanski, *J. Mol. Struct.*, 2000, **555**, 1.
29 T. Nakayama, Y. Amijima, K. Ibuki and K. Hamanoue, *Rev. Sci. Instrum.*, 1997, **68**, 436.
30 M. Ziolek, M. Lorenc and R. Naskrecki, *Appl. Phys. B*, 2001, **72**, 843.
31 M. Lorenc, M. Ziolek, R. Naskręcki, J. Karolczak, J. Kubicki and A. Maciejewski, *Appl. Phys. B*, 2002, **74**, 19.
32 S. R. Meech and D. Philips, *J. Photochem.*, 1983, **23**, 193.
33 D. Zhong, A. Douhal and A. H. Zewail, *Proc. Natl. Acad. Sci. USA*, 2000, **97**, 14056.
34 W. G. Chen and M. S. Braiman, *Photochem. Photobiol.*, 1991, **54**, 905.
35 S. Yamaguchi and H. Hamaguchi, *Chem. Phys. Lett.*, 1998, **287**, 694.
36 N. P. Ernsting, S. A. Kovalenko, T. Senyushkina, J. Saam and V. Farztdinov, *J. Phys. Chem. A*, 2001, **105**, 3443.

37 M. Rini, A. Kummrow, J. Dreyer, E. T. J. Nibbering and T. Elsaesser, *Faraday Discuss.*, 2002, **122**, 27.
38 S. Lochbrunner, A. J. Wurzer and E. Riedle, *J. Chem. Phys.*, 2000, **112**, 10699.
39 S. Lochbrunner, A. J. Wurzer and E. Riedle, *J. Phys. Chem. A*, 2003, **107**, 10580.
40 R. de Vivie-Riedle, V. De Waele, L. Kurtz and E. Riedle, *J. Phys. Chem. A*, 2003, **107**, 10591.
41 C. Chudoba, E. Riedle, M. Pfeiffer and T. Elsaesser, *Chem. Phys. Lett*, 1996, **263**, 622.
42 C. Chudoba, S. Lutgen, T. Jentzsch, E. Riedle, M. Woerner and T. Elsaesser, *Chem. Phys. Lett*, 1995, **240**, 35.
43 M. C. Zerner, J. E. Ridley, A. D. Bacon, W. D. Edwards, J. D. Head, J. McKelvey, J. C. Culberson, P. Knappe, M. G. Cory, B. Weiner, J. D. Baker, W. A. Parkinson, D. Kannis, J. Yu, N. Roesch, M. Kotzian, T. Tamm, M. M. Karelson, X. Zheng, G. Pearl, A. Broo, K. Albert, J. M. Cullen, J. Li, G. D. Hawkins, J. D. Thompson, D. A. Liotard, C. J. Cramer and D. G. Truhlar, *ZINDO–MN1.1, Quantum Theory Project*, Univ. of Florida, Gainesville, and Dept. of Chemistry, Univ. of Minnesota, Minneapolis, 2000.
44 J. E. Ridley and M. C. Zerner, *Theor. Chim. Acta*, 1973, **32**, 111.
45 M. Rini, J. Dreyer, E. T. J. Nibbering and T. Elsaesser, *Chem. Phys. Lett.*, 2003, **374**, 13.
46 J. R. Choi, S. Ch. Jeoung and D. W. Cho, *Chem. Phys. Lett.*, 2004, **385**, 384.
47 A. Douhal, F. Lahmani and A. H. Zewail, *Chem. Phys.*, 1996, **207**, 477.